

Fast Potentiometric CO₂ Sensor for High-resolution *In situ* Measurements in Fresh Water Systems

Rohini Athavale^{1, 2†*}, Nadezda Pankratova^{3, 4‡}, Christian Dinkel¹, Eric Bakker³, Bernhard Wehrli^{1, 2},
Andreas Brand^{1, 2}

¹Eawag – Swiss Federal Institute of Aquatic Science and Technology, Department of Surface Waters Research and
Management, Seestrasse 79, CH-6047 Kastanienbaum, Switzerland.

²Institute of Biogeochemistry and Pollutant Dynamics, ETH Zurich, Universitätsstrasse 16, CH-8092 Zürich,
Switzerland.

³Department of Inorganic and Analytical Chemistry, University of Geneva, Quai E.-Ansermet 30, 1211 Geneva,
Switzerland.

⁴Integrated Systems Laboratory (LSI), Swiss Federal Institute of Technology Lausanne (EPFL), CH-1015
Lausanne, Switzerland.

[†] Both authors contributed equally

*Corresponding Author

E-mail: rohini.athavale@eawag.ch

Phone Number: +41 587655633

ABSTRACT

We present a new potentiometric sensor set up and a calibration protocol for *in situ* profiling of
CO₂ with high temporal and spatial resolution in fresh water lakes. The principle of this sensor
system is based on the measurement of EMF between two solid contact ion selective electrodes
(SC-ISEs), a hydrogen ion selective and a carbonate selective sensor. Since the setup relies on

SC-ISEs, it is insensitive to changes in the pressure, thus suitable for *in situ* studies. Also as it offers a response time ($t_{95\%}$) of <10s it allows profiling applications at high spatial resolution. The proposed optimum *in situ* protocol accounts for the continuous drift and change in offset that remains a challenge during profiling in natural waters. The fast response resolves features that are usually missed by standard methods like the classical Severinghaus CO₂ probe. In addition, the insensitivity of the presented setup to dissolved sulfide allows also measurements in anoxic zones of eutrophic systems. Highly resolved CO₂ concentration profiles obtained as a result of a novel and robust SC-ISE set up along with the developed optimum *in situ* protocol allow the close investigation of hotspots for biogeochemical processes such as mineralization and primary production in the water column and help improving estimates for CO₂ turnover in freshwater systems.

INTRODUCTION

In the face of increasing anthropogenic perturbations to the global carbon cycle, the processes underlying the global carbon budget, including CO₂ turnover and its exchange between inland waters and the atmosphere, need to be thoroughly characterized.¹ Since many of these processes, e.g., aerobic methane oxidation processes acting as methane filters, often are confined to small spatial scales in lakes, a measurement technique for CO₂ with high spatial resolution would be helpful.^{2, 3} In addition, it is important to understand the occurrence of biogeochemical hotspots of photosynthesis and respiration and their impact on the concentration of dissolved CO₂.⁴ High-resolution *in situ* measurements are required to locate and quantify these sources and sinks.⁵

In situ measurements of CO₂ can be achieved by several indirect and direct methods. The indirect methods involve measurement of parameters like pH, total alkalinity (TA), dissolved inorganic carbon (DIC) by laboratory-based techniques.⁶ Biases and errors associated with

calculating CO₂ from pH and alkalinity values currently limit the precision of estimates of CO₂ emissions from inland waters because they neglect the presence of other organic and inorganic buffer systems.^{1, 7} Some of the lab based techniques have been further developed to be suitable for *in situ* measurements as reported by several studies in marine environments e.g., *in situ* spectrophotometric measurements of DIC and pH and TA,⁸⁻¹⁰ as well as mass spectrometric approaches for *in situ* and on-site measurements.^{11, 12} However, the sampling, reaction or equilibration time required in these setups spans over several minutes. Response time in minutes does not favor high spatiotemporal measurement demands of inland waters especially lakes.^{13, 14} Direct *in situ* measurements of dissolved CO₂ are traditionally obtained by the Severinghaus probe¹⁵ or with infrared spectroscopy (NDIR sensing element).¹⁶ The Severinghaus probe (CO₂-SH probe) is inexpensive and easy to handle. It consists of a pH-sensing element in contact with a bicarbonate buffer, which is separated from the sample solution by a gas permeable membrane. Since the equilibrium between bulk and sample phases is established by diffusion, the probe signal needs several minutes to stabilize. This slow response time is a major drawback in applications that require rapid monitoring.^{15, 17, 18} Also, the gas permeable membrane is not only selective for CO₂ but also allows diffusion of H₂S, which then alters pH of the internal buffer and causes interference in the sulfidic deep waters, typical of stratified, eutrophic lakes.^{17, 19, 20}

Potentiometric sensing offers a promising alternative for *in situ* high-resolution measurements.²¹ The principle of the presented CO₂ setup is based on the measurement of electromotive force (EMF) of a pH electrode against a carbonate electrode without using any reference element.²² As it is demonstrated by Xie et al.²² the following equations illustrate the mechanism of the set up. Considering the acid dissociation equilibria of dissolved carbon dioxide in water,



activity of dissolved CO₂ is linked with that of carbonate and hydrogen ion according to equation (B) and (C).

$$a_{\text{CO}_2} = \frac{a_{\text{CO}_3^{2-}} (a_{\text{H}^+})^2}{K_{a1} K_{a2}} \quad (\text{B})$$

Where K_{a1} and K_{a2} are two acid dissociation constants for dissolved CO₂. Combined set up comprising of a hydrogen ion and a carbonate selective electrode gives,

$$E_{\text{comb}} = K' + \frac{S}{2} \log (a_{\text{CO}_3^{2-}} (a_{\text{H}^+})^2) = K + \frac{S}{2} \log a_{\text{CO}_2} \quad (\text{C})$$

K and K' being constants that vary with the inner solution composition of the electrodes. As no gas permeable membrane is involved, no interference from H₂S gas is expected unlike the Severinghaus probe. A highly selective carbonate ion selective electrode (ISE) based on a new class of carbonate ionophores was reported by the group of Nam and Cha.²³ Selectivity studies on such a carbonate ISE have shown that Cl⁻ and HS⁻ does not interfere even at high concentrations, which makes the ISE suitable for use in natural waters and ²²⁻²⁶ Xie et al.²² successfully tested the principle of this approach in the laboratory.

In this study, we present an *in situ* application and validation of a potentiometric sensing principle for dissolved CO₂ in the water column of a temperate lake. *In situ* application where profiling with high resolution with respect to space and time, across depths is involved, a pressure insensitive sensor setup is required. We utilized the inherently pressure proof, all solid state, solid contact ion selective electrodes (SC ISEs) in a double layer design. The utilized double layer design¹⁴ with a carbon nanotube based layer as a solid contact for both H⁺ and CO₃²⁻ selective SC ISEs imparted sulfide insensitivity and a methacrylic co-polymer as membrane matrix for H⁺, which added to the insensitivity towards sulfide.²¹ We also developed an optimized *in situ* calibration protocol based on earlier findings^{14, 21} that identified and corrected for changes in electrode offsets and drifts during profiling in water columns of lakes with strong chemical gradients. Finally, we tested the advantages of our approach over a

classical Severinghaus CO₂ probe for high resolution depth profiling in fresh water lakes. For the field tests, we selected the eutrophic Lake Rotsee (Switzerland), which has steep redox and solute gradients that are challenging for profiling applications.

MATERIALS AND METHODS

Sensor design

The sensor system consisted of an H⁺ ion selective SC-ISE measured against a CO₃²⁻ selective SC-ISE in a potentiometric set up without use of any reference element. Functionalized multiwalled carbon nanotubes (f-MWCNTs) were used as a transducing material in a double layer (DL) design to fabricate both SC-ISEs. Carboxylic-acid groups were created on the surface of the MWCNTs by oxidation followed by amide formation with octadecylamine to yield f-MWCNTs.²⁷ Nanotubes were dispersed in tetrahydrofuran by slight sonication to form a homogeneous dispersion which was then drop cast on a polished mini glassy carbon electrode (GCE, Metrohm AG, Switzerland) surface to form a uniform transducing layer. Separate SC-ISEs for CO₃²⁻ and H⁺ were fabricated by casting an ion selective membrane matrix on top of the f-MWCNT layer. A methacrylic co-polymer (MMA-DMA) based membrane, was cast for hydrogen ion selective²¹ and a polyvinyl chloride (PVC) based membrane matrix for the carbonate selective SC-ISE²² (details in SI). The sensor quality was assessed by checking for Nernstian response (Figure1), insensitivity towards redox, long-term stability, water-layer formation and sulfide insensitivity (see SI).

Field site

Lake Rotsee, an eutrophic lake in Central Switzerland was chosen as the study site. It has a surface area of 0.48 km², and an average and maximum depth of 9 and 16 m, respectively. A strong chemocline is located between 8-11m during the stratification period, which starts in

spring and holds until late autumn. This eutrophic lake exhibits steep redox and nutrient gradients across the oxycline during the stratification period.²⁸ The profiling tests were performed in November 2017 i.e. at the end of the summer stratification when accumulation of CO₂ and other mineralization products reached maximum concentrations in the hypolimnion. Convective mixing in the surface waters maintained the steep gradients near the thermocline. These physicochemical conditions in the lake allowed for testing the sensors at a range of concentrations with sharp changes in analyte concentrations and redox conditions.

Set up for in situ profiling

The potentiometric CO₂ sensing system was integrated into our custom-built Profiling Ion Analyzer (PIA) (SI Figure S4).¹⁴ PIA consisted of a cubic aluminum frame with dimensions 50×50×60 cm. On top of this frame, a data-recording unit (a Z-Brain data logger from Schmid Engineering Systems AG, Switzerland) with its power supply was placed. During the onboard calibration and *in-situ* deployment, the SC-ISEs were connected to waterproof, galvanically isolated potentiometric-sensing units in order to preclude cross talk. For signal stability and noise rejection an instrumentation amplifier (Burr-Brown, Model INA116, from Texas Instruments, Dallas, TX, USA) with ultra low input bias current (3 fA) and a high common-mode rejection (84 dB) was utilized. The EMF for each indicator H⁺ selective SC-ISE (mini glassy carbon electrode, Metrohm AG, Switzerland) was measured against CO₃²⁻ selective SC-ISE (mini glassy carbon electrode, Metrohm AG, Switzerland) with a platinum wire as common solution ground (INA116 datasheet, BURR-BROWN).²⁹ PIA was equipped with additional sensors for characterization of the water column, specifically a CTD probe for measuring conductivity, temperature and depth (XR-420, RBR Ltd., Canada) and needle type optodes for recording dissolved oxygen concentrations (PreSens - Precision Sensing GmbH, Germany). A syringe sampler integrated into the PIA system (KC Denmark) at the center of the cubic frame allowed retrieval of 12 water samples at different depths with a volume of 60 mL along with simultaneous recording of EMF by ISEs and all other integrated measurements. PIA was

149 deployed with a electric winch in the lake with a constant profiling speed of 5 mm/ s and syringe
150 samples were taken simultaneously during the profile recording at different depth intervals. A
151 Severingshaus gas sensing probe for CO₂ was also accommodated in the whole set up (Idronaut
152 S.r.l, I-20047 Brugherio, Italy).

153 *Laboratory analysis*

154 Dissolved inorganic carbon (DIC) was sampled in 12 mL pre-evacuated DIC exetainers VWR
155 International GmbH)) after filtering through 0.2 µM cellulose acetate syringe filter (VWR
156 International GmbH) on board and measured by TOC analyser (SHIMADZU, Switzerland).
157 Total sulfide was determined by spectrophotometric analysis following Cline et al.³⁰ (SI), and
158 concentrations of major cations (NH₄⁺, K⁺, Ca²⁺, Mg²⁺, Na⁺) and anions (Cl⁻, SO₄²⁻, NO₃⁻) in the
159 water column were measured by ion chromatography (Metrohm AG, Switzerland) (Table S1).

160 *Calculation of dissolved CO₂ activity*

161 The DIC as well as dissolved ion concentrations were measured on syringe samples. A CTD
162 probe recorded pH and temperature *in situ* in parallel to syringe sampling .These results were
163 compiled as an input to the PHREEQC program for speciation calculations³¹. The activity of
164 dissolved CO₂ was obtained as output and was further used for the *in situ* calibrations.

165 *Optimization of calibration protocol*

166 In order to have a optimum calibration protocol with minimum sampling efforts we evaluated
167 different calibration schemes. Table 1 summarizes four strategies for calibration and
168 corresponding values of calibration parameters obtained via these strategies. Specifically in
169 Table 1a, the first scheme is based on onboard calibration before the deployment to check for
170 the performance of already mounted sensors on PIA in terms of slope and intercept. The
171 following *in situ* strategies involved *in situ* sampling with the syringe sampler (integrated in
172 PIA) during ongoing profiling to consider for drift and changes in temperature experienced

during profiling in the water column. For optimization of the calibration protocol (Scheme 3, Table 1a) both onboard and *in situ* calibration efforts were blend together to consider drift, interferences from other ions and temperature changes as additional factors to the standard calibration parameters namely slope and intercept.

Onboard calibration was performed on the boat just before lowering the PIA system in the lake for *in situ* measurements. Three buffer solutions with different dissolved CO₂ concentrations coinciding with the typical concentrations in the lake were used for onboard calibration: 10mM Tris buffer solutions with 5mM bicarbonate and 150μM chloride was tuned with sulfuric acid to different pH values of 7.52, 8.04 and 8.74 to attain three buffer solutions with a_{CO_2} 302μM, 95μM and 19μM respectively. The CO₂-SH probe was checked for the Nernstian response (Figure 1c) using similar buffer solutions in the laboratory prior to the field deployment.

In situ calibration, where the obtained raw EMF profile can be corrected for drift and interference from other ions has been proven essential to obtain accurate high-resolution concentration profiles with ISEs.^{14, 21} This published *in situ* calibration protocols in Eq. 1 establishes the basic logic of in situ calibration strategy in general and considers the value of EMF and the corresponding concentration of analyte at all sampling points to derive the value of the slope S [mV/decade], drift, d [mV/s] and intercept, E⁰ [mV] using least square optimization:

$$\log (a_a + a_b \times K_{a,b}^{pot}) = (EMF - (d \times t) - E^0) / S \quad (\text{Eq. 1}),$$

where EMF is expressed in mV and t is the time passed since the start of profiling [s], a_a is the activity of the ion of interest; a_b is the activity of an interfering ion [mol/l]. Owing to the use of highly selective ionophores for preparation of ion selective membrane (ISM) for both for H⁺ and CO₃²⁻^{23, 25-27, 32} and significantly low concentrations of relevant interfering ions (Table S1) in the lake water column, there was no necessity to correct for the interference by the factor $c_b \times K_{a,b}^{pot}$. The temperature affected the slope (~10%) of the divalent CO₃²⁻ when tested over a

range of temperatures typically found in the lake. Therefore, the temperature dependence of S was explicitly included in solving for a_a . T is temperature in K and T_0 is temperature at the beginning of profiling in Eq. 2:

$$\log a_a = (\text{EMF} - (d \times t) - E^0) / ((S/T_0) \times T) \quad (\text{Eq. 2}),$$

The Eq. 2 optimized with respect to drift, interferences and temperature compensation was further utilized for calibrating the sensor setup for dissolved CO_2 i.e., combined pH and carbonate SC ISE. These calibration parameters were further used to convert the high resolution EMF profiles obtained in the water column to values for activity of dissolved CO_2 .

Response time

To assess how fast the CO_2 -ISE couple responds to the changes in the activity of CO_2 under *in situ* conditions, an *in situ* response time test was carried out. We chose two water depths at 6.5m and 8.5m, based on the profiles available on board. The whole PIA set up with ISE couples and SH type probe was then taken to 6.5m and rested there for ~10min to observe the stable response and was driven to the next point i.e. 8.5m with the speed 5cm/s which is 10 times the normal profiling speed.

RESULTS AND DISCUSSION

The CO_2 -ISE couple utilizes an all solid-state design inherently insensitive to pressure, which is a prerequisite for *in situ* measurements in the water column. Both CO_3^{2-} and H^+ selective SC-ISEs show close to Nernstian response with values of slopes -27.2mV/decade (LOD ~2 μM) and 56.3 mV/decade (LOD ~1 nM), respectively in the laboratory (Figure 1a). With alkalinity values during the stratification period ranging from around 1.5- 3.5 mmol/l and pH between 7.2-8.2 the bicarbonate ion predominates in the bicarbonate-carbonate equilibria in the water column. With the lower detection limits of the presented ISEs especially carbonate selective

sensor in micro molar range allows measurements in the given pH range in Lake Rotsee with lowest carbonate concentrations above the LOD of carbonate sensor. Although functioning at lower pH values than pK_{a1} of the CO_2 system has been reported²² it might depend on the TIC or alkalinity of the system and can limit applications at carbonate concentrations lower than 1 μM . A sulfide sensitivity test up to 100 μM dissolved total sulfide in a buffered solution (Tris buffer pH 8) (SI, Figure S1) did not show any drift due to sulfide interference in the laboratory which can be attributed to choice of a DL design employing f-MWCNTs as a transducer. The use of carbon nanotubes also makes the CO_2 -ISE couple light insensitive against variable light conditions in the field.²¹ The water layer test and redox sensitivity³³⁻³⁵ did not show any significant changes in EMF (Table S2). The response time ($t_{95\%}$) of both the SC-ISEs and the CO_2 ISE-couple was estimated according to IUPAC conventions³⁶ and was found to be <10 s. Hence, the fast responding, stable, insensitive to sulfide and to the light conditions and with LODs low enough for measurements in natural waters, puts forward the CO_2 -ISE couple as a suitable candidate for *in situ* profiling in lakes.

We also observed a Nernstian response for both CO_2 ISE-couples during onboard calibration on PIA and for CO_2 -SH probe in the laboratory prior to the deployment (Figures 1b and 1c). The interaction of the lake matrix with the membrane surface, leaching of membrane components may cause a drift in the signal and can impart slow changes in the intercept (E^0). However, drift experienced by the sensors (SI Figure S2, Table 1) and the changes in intercept¹⁴ inherent to complex matrices with dissolved and particulate organics and inorganics could not be controlled by calibration with buffer solution onboard only. To compensate for the observed drift and changes in the intercept empirically, parallel sampling during ongoing EMF profiling followed by evaluation of the chemical composition is reported to be necessary.¹⁴ A single value for a parallel drift³⁴ and intercept was obtained for each EMF profile by fitting $\log a_a$ to Eq. 2 using least square optimization. The slopes obtained from onboard calibration for CO_2 -ISE couple and from the laboratory calibration for CO_2 -SH (Table 1) were taken over for the

different *in situ* calibration strategies, as the *in situ* interference correction was not needed for the slope. Calibration scheme 2 as described in Table 1a utilized the value of slope obtained by onboard calibration and values for drift and intercept for both sensor sets were obtained by fitting $\log a_a$ to Eq. 2 by least square optimization only for drift and intercept (table 1b and 1c). To further reduce the effort of sampling at as many depth points as possible (10 points in the case of Scheme 2) to derive the values of drift and intercept, scheme 3 used only two depth points at the beginning and end of the profile yielded a better fit of the activity profile to the syringe concentrations for dissolved CO₂ compared to scheme 2 (Figure 2). Due to the reduced sampling effort, calibration scheme 3 was considered as the optimal strategy. Calibration scheme 4 corresponded to the published strategy^{12, 13} in this of case all the calibration parameters were derived by fitting $\log a_a$ to Eq. 2 using least square optimization by varying d , E^0 and S considering all sampling points. The resulting values of slightly super-Nernstian slopes (close to scheme 3) for both couples confirm that the use of slope values from on-board calibration without interference correction was suitable.

Similar calibration protocols were carried out also for the CO₂-SH probe (Table 1d, SI Figure S3). Except that the probe needed to rest at two sampling points for ~10min to record its stable response considered to calculate drift and intercept. Water depths of 6.5 m and 8.5 m were chosen for this purpose. The value of slope was carried forward from the laboratory analysis with the Tris buffer solutions. The failure of the CO₂-SH probe to reproduce the syringe concentrations (SI Figure S3) is a result of its slow response to changes in the concentration. Also, the gas permeable membrane in CO₂-SH probe, is not selective to CO₂ but allows contamination with other gases such as H₂S that alters the pH of the buffer solution and leads to measurements that overestimate CO₂ (SI Figure S1).

The temporal response

An experiment across the oxycline with two stops compares the performance of both CO₂-ISE couple and SH-CO₂ probe (Figure 3). At 6.5 m water depth CO₂ concentrations were low due

to photosynthetic activity and convective mixing. Stable response was at this depth for both sensors with a slight drift for SH-CO₂ probe. In a next step, the whole PIA setup was lowered to the depth point at 8.5m with 10 times the normal speed (4 cm s⁻¹). The travel time between the two depths was ~50 s. In this short time interval, a sharp jump in ΔEMF/slope for CO₂-ISE couple indicates that the sensing system responded rapidly to an activity change of $\log a_{CO_2}$ of 0.78 units which matches well with the immediate jump of 0.8 in ΔEMF/slope for the CO₂-ISE couple. The fluctuations in the response of CO₂-ISE couple seen at 8.5m could be explained by the location of this sampling point just at the end of the steep oxycline where any depth fluctuations cause significant changes in dissolved CO₂ activity. In contrast, the response of CO₂-SH probe shows a very smooth response curve which extends for >5min until it is stable. Thus, the steep concentration changes are missed by CO₂-SH probe owing to its slow response.

Embedded details in highly resolved CO₂ profiles

In situ high-resolution profiles of the activity of dissolved CO₂ from 2 to 12 m in Lake Rotsee taken at a profiling speed of 0.5cm/s show distinct features which can be linked to other physicochemical parameters in order to infer the governing biogeochemical processes (Figure 4). During profiling, the epilimnion had rather uniform O₂ concentrations (250 μM) down to 8m. The photosynthetic utilization in the epilimnion tends to reduce the CO₂ content (26 μM) above 8 m. The CO₂ profiles obtained by the ISE couples and the SH probe agreed with the syringe concentrations down to the oxycline. Below the oxycline a strong increase in CO₂ concentration was observed due to its accumulation in the anoxic hypolimnion fed by inputs from the sediments and mineralization processes in the water column. In general, the CO₂ profiles obtained with the ISE-couple showed detailed features between the sampling points, which indicates distinct biogeochemical activity at the cm scale. For instance, at depth 8.5m a small hump extending over ~ 20 cm in the CO₂ profile was observed which was totally missed by the CO₂-SH probe owing to its slow response. This small feature coincided with a peak in the turbidity profile, which typically indicates a layer with high cell numbers that accumulated

at the upper end of the thermocline and performed oxic respiration processes and photosynthesis at low-light conditions. The occurrence of this phenomena has been described for Lake Rotsee by Brand et al.²⁸ and Oswald et al.³⁷

In summary, we were able to develop an *in situ* set up for dissolved CO₂ measurements at high temporal and spatial resolution. The optimized *in situ* calibration protocol allows reducing sampling efforts for reliable results. Careful conditioning steps are recommended as essential to achieve reliable response close to LOD as determined in the laboratory. The *in situ* sampling and calibration steps could not be avoided in the field for the determination of drift and optimum offset potentials. As only two sampling points are proposed to be sufficient for compensating for the drift and changes in offset potentials according to the optimized calibration protocol, users may also employ other sampling devices than a syringe sampler e.g., a Niskin bottle if triggered for sampling at the coinciding depth and time point as measurement of EMF of the set up. The response time of few seconds offered by the CO₂-ISE setup opens the perspective to capture the fast dynamic of biogeochemical processes and to map hot spots of CO₂ production. The sulfide insensitivity observed in this field application with up to 100 µM total sulfides facilitates using the CO₂-ISE in anoxic waters without interference. This simple yet elegant potentiometric sensing system for CO₂ could serve as an effective tool for studying biogeochemical processes occurring at small scales in freshwater systems.

Supporting Information: Experimental section with materials and chemicals, sensor fabrication, laboratory tests, sulfide sensitivity test (Figure S1), depth profile of raw and drift corrected ΔEMF (Figure S2), depth profiles of activity of dissolved CO₂ obtained by CO₂-SH probe with different calibration schemes (Figure S3), *in-situ* profiling set up (Figure S4), selectivity coefficients for ion selective membranes and mean concentrations of relevant ions in the lake water column (Table S1), performance of SC-ISEs during laboratory tests (Table S2).

326

327 ACKNOWLEDGMENTS

328 The authors are grateful for the financial support from the Swiss National Science Foundation
329 (SNF Grant 147654). We would like to thank Yuan Danjing for his help in synthesis of f-
330 MWCNTs in the laboratory.

- 332 1. Raymond, P. A.; Hartmann, J.; Lauerwald, R.; Sobek, S.; McDonald, C.; Hoover, M.; Butman,
333 D.; Striegl, R.; Mayorga, E.; Humborg, C.; Kortelainen, P.; Dürr, H.; Meybeck, M.; Ciais, P.; Guth, P.,
334 Global carbon dioxide emissions from inland waters. *Nature* **2013**, *503*, 355.
- 335 2. Milucka, J.; Kirf, M.; Lu, L.; Krupke, A.; Lam, P.; Littmann, S.; Kuypers, M. M. M.; Schubert, C.
336 J., Methane oxidation coupled to oxygenic photosynthesis in anoxic waters. *The Isme Journal* **2015**, *9*,
337 1991.
- 338 3. Jan, B.; Helge, N.; B., W. C.; Jakob, Z.; J., S. C.; K., K. M.; L., V. M.; Carmen, H.; F., L. M., Micro-
339 aerobic bacterial methane oxidation in the chemocline and anoxic water column of deep south-
340 Alpine Lake Lugano (Switzerland). *Limnol Oceanogr* **2014**, *59*, (2), 311-324.
- 341 4. Wetzel, R. G., The inorganic carbon complex. In *Limnology (Third Edition)*, Academic Press:
342 San Diego, 2001; pp 187-204.
- 343 5. Stocker, R., Marine Microbes See a Sea of Gradients. *Science* **2012**, *338*, (6107), 628-633.
- 344 6. Byrne, R. H., Measuring Ocean Acidification: New Technology for a New Era of Ocean
345 Chemistry. *Environ Sci Technol* **2014**, *48*, (10), 5352-5360.
- 346 7. Abril, G.; Bouillon, S.; Darchambeau, F.; Teodoru, C. R.; Marwick, T. R.; Tamoo, F.; Ochieng
347 Omengo, F.; Geeraert, N.; Deirmendjian, L.; Polsenaere, P.; Borges, A. V., Technical Note: Large
348 overestimation of CO_2 calculated from pH and alkalinity in acidic, organic-rich
349 freshwaters. *Biogeosciences* **2015**, *12*, (1), 67-78.
- 350 8. Liu, X.; Byrne, R. H.; Adornato, L.; Yates, K. K.; Kaltenbacher, E.; Ding, X.; Yang, B., In Situ
351 Spectrophotometric Measurement of Dissolved Inorganic Carbon in Seawater. *Environ Sci Technol*
352 **2013**, *47*, (19), 11106-11114.
- 353 9. Wang, Z. A.; Sonnichsen, F. N.; Bradley, A. M.; Hoering, K. A.; Lanagan, T. M.; Chu, S. N.;
354 Hammar, T. R.; Camilli, R., In Situ Sensor Technology for Simultaneous Spectrophotometric
355 Measurements of Seawater Total Dissolved Inorganic Carbon and pH. *Environ Sci Technol* **2015**, *49*,
356 (7), 4441-4449.
- 357 10. Martz, T. R.; Dickson, A. G.; DeGrandpre, M. D., Tracer Monitored Titrations: Measurement
358 of Total Alkalinity. *Analytical chemistry* **2006**, *78*, (6), 1817-1826.
- 359 11. Bell, R. J.; Short, R. T.; Byrne, R. H., In situ determination of total dissolved inorganic carbon
360 by underwater membrane introduction mass spectrometry. *Limnology and Oceanography: Methods*
361 **2011**, *9*, (4), 164-175.
- 362 12. Brennwald, M. S.; Schmidt, M.; Oser, J.; Kipfer, R., A Portable and Autonomous Mass
363 Spectrometric System for On-Site Environmental Gas Analysis. *Environ Sci Technol* **2016**, *50*, (24),
364 13455-13463.
- 365 13. Kirf, M. K.; Dinkel, C.; Schubert, C. J.; Wehrli, B., Submicromolar Oxygen Profiles at the Oxic-
366 Anoxic Boundary of Temperate Lakes. *Aquat Geochem* **2014**, *20*, (1), 39-57.
- 367 14. Athavale, R.; Kokorite, I.; Dinkel, C.; Bakker, E.; Wehrli, B.; Crespo, G. A.; Brand, A., In Situ
368 Ammonium Profiling Using Solid-Contact Ion-Selective Electrodes in Eutrophic Lakes. *Analytical*
369 *chemistry* **2015**, *87*, (24), 11990-11997.
- 370 15. Severinghaus, J. W.; Bradley, A. F., Electrodes for Blood pO₂ and pCO₂ Determination.
371 *Journal of Applied Physiology* **1958**, *13*, (3), 515-520.
- 372 16. Fietzek, P.; Kötzinger, A., Optimization of a Membrane-Based NDIR Sensor for Dissolved
373 Carbon Dioxide. *ESA, Publication WPP-306 2010 Venice, Italy, 21-25 September 2009, Hall, J.,*
374 **Harrison D.E. & Stammer, D., Eds.**
- 375 17. Suzuki, H.; Arakawa, H.; Sasaki, S.; Karube, I., Micromachined Severinghaus-Type Carbon
376 Dioxide Electrode. *Analytical chemistry* **1999**, *71*, (9), 1737-1743.
- 377 18. Wang, Z. A.; Liu, X.; Byrne, R. H.; Wanninkhof, R.; Bernstein, R. E.; Kaltenbacher, E. A.; Patten,
378 J., Simultaneous spectrophotometric flow-through measurements of pH, carbon dioxide fugacity, and
379 total inorganic carbon in seawater. *Anal Chim Acta* **2007**, *596*, (1), 23-36.
- 380 19. Morf, W. E.; Mostert, I. A.; Simon, W., Time response of potentiometric gas sensors to
381 primary and interfering species. *Analytical chemistry* **1985**, *57*, (6), 1122-1126.

20. Lopez, M. E., Selectivity of the potentiometric carbon dioxide gas-sensing electrode. *Analytical chemistry* **1984**, *56*, (13), 2360-2366.
21. Athavale, R.; Dinkel, C.; Wehrli, B.; Bakker, E.; Crespo, G. A.; Brand, A., Robust Solid-Contact Ion Selective Electrodes for High-Resolution In Situ Measurements in Fresh Water Systems. *Environmental Science & Technology Letters* **2017**, *4*, (7), 286-291.
22. Xie, X.; Bakker, E., Non-Severinghaus potentiometric dissolved CO₂ sensor with improved characteristics. *Analytical chemistry* **2013**, *85*, (3), 1332-6.
23. Choi, Y. S.; Lvova, L.; Shin, J. H.; Oh, S. H.; Lee, C. S.; Kim, B. H.; Cha, G. S.; Nam, H., Determination of Oceanic Carbon Dioxide Using a Carbonate-Selective Electrode. *Analytical chemistry* **2002**, *74*, (10), 2435-2440.
24. Lee, H. J.; Yoon, I. J.; Yoo, C. L.; Pyun, H.-J.; Cha, G. S.; Nam, H., Potentiometric Evaluation of Solvent Polymeric Carbonate-Selective Membranes Based on Molecular Tweezer-Type Neutral Carriers. *Analytical chemistry* **2000**, *72*, (19), 4694-4699.
25. Beer, D. d.; Bissett, A.; Wit, R. d.; Jonkers, H.; Köhler-Rink, S.; Nam, H.; Kim, B. H.; Eickert, G.; Grinstain, M., A microsensor for carbonate ions suitable for microprofiling in freshwater and saline environments. *Limnology and Oceanography: Methods* **2008**, *6*, (10), 532-541.
26. Pankratova, N.; Crespo, G. A.; Afshar, M. G.; Crespi, M. C.; Jeanneret, S.; Cherubini, T.; Tercier-Waeber, M.-L.; Pomati, F.; Bakker, E., Potentiometric sensing array for monitoring aquatic systems. *Environmental Science: Processes & Impacts* **2015**, *17*, (5), 906-914.
27. Yuan, D.; Anthi, A. H. C.; Ghahraman Afshar, M.; Pankratova, N.; Cuartero, M.; Crespo, G. A.; Bakker, E., All-Solid-State Potentiometric Sensors with a Multiwalled Carbon Nanotube Inner Transducing Layer for Anion Detection in Environmental Samples. *Analytical chemistry* **2015**, *87*, (17), 8640-8645.
28. Brand, A.; Bruderer, H.; Oswald, K.; Guggenheim, C.; Schubert, C. J.; Wehrli, B., Oxygenic primary production below the oxycline and its importance for redox dynamics. *Aquat Sci* **2016**, *78*, (4), 727-741.
29. Müller, B.; Maerki, M.; Dinkel, C.; Stierli, R.; Wehrli, B., In Situ Measurements in Lake Sediments Using Ion-Selective Electrodes with a Profiling Lander System. In *Environmental Electrochemistry*, American Chemical Society: 2002; Vol. 811, pp 126-143.
30. Cline, J. D., Spectrophotometric determination of hydrogen sulfide in natural waters. *Limnology and Oceanography* **1969**, *14*, (3), 454-458.
31. Parkhurst, D. L., *User's guide to PHREEQC: a computer program for speciation, reaction-path, advective-transport, and inverse geochemical calculations*. Lakewood, Colo. : U.S. Dept. of the Interior, U.S. Geological Survey ; Denver, CO : Earth Science Information Center, Open-File Reports Section [distributor], 1995.: 1995.
32. Crespo, G. A.; Gugs, D.; Macho, S.; Rius, F. X., Solid-contact pH-selective electrode using multi-walled carbon nanotubes. *Anal Bioanal Chem* **2009**, *395*, (7), 2371-2376.
33. Fibbioli, M.; Bandyopadhyay, K.; Liu, S.-G.; Echegoyen, L.; Enger, O.; Diederich, F.; Buhlmann, P.; Pretsch, E., Redox-active self-assembled monolayers as novel solid contacts for ion-selective electrodes. *Chem Commun* **2000**, (5), 339-340.
34. Lindner, E.; Gyurcsanyi, R. E., Quality control criteria for solid-contact, solvent polymeric membrane ion-selective electrodes. *Journal of Solid State Electrochemistry* **2009**, *13*, (1), 51-68.
35. Mousavi, Z.; Teter, A.; Lewenstam, A.; Maj-Zurawska, M.; Ivaska, A.; Bobacka, J., Comparison of Multi-walled Carbon Nanotubes and Poly(3-octylthiophene) as Ion-to-Electron Transducers in All-Solid-State Potassium Ion-Selective Electrodes. *Electroanal* **2011**, *23*, (6), 1352-1358.
36. Lindner, E.; Toth, K.; Pungor, E., Definition and determination of response time of ion selective electrodes. *Pure Appl Chem* **1986**, *58*, (3), 469-479.
37. Oswald, K.; Milucka, J.; Brand, A.; Littmann, S.; Wehrli, B.; Kuypers, M. M. M.; Schubert, C. J., Light-Dependent Aerobic Methane Oxidation Reduces Methane Emissions from Seasonally Stratified Lakes. *PLOS ONE* **2015**, *10*, (7), e0132574.

433

434

435 TABLES

436 **Table 1.**

437 (a) Different calibration strategies optimal scheme in blue.

Description	
1	On-board Calibration
2	<i>In situ</i> calibration, slope value from on board calibration; drift and intercept fitted from all sampling points
3	<i>In situ</i> calibration, slope value from on board calibration; drift and intercept obtained from two (1 st and last) sampling points
4	<i>In situ</i> calibration, slope value, drift and intercept obtained from fit to all sampling points

438

439 (b) Calibration schemes with corresponding parameters for CO₂-ISE couple 1, optimal scheme in
440 blue

CO ₂ -ISEcouple 1		Slope (mV/decade)	Intercept (mV)	Drift (mV/s)
	1	31.06	-65.36	-
Calibration Type*	2	31.06	-45.94	0.005
	3	31.06	-45.69	0.004
	4	32.53	-38.76	0.003

441

442 (c) Calibration schemes with corresponding parameters for CO₂-ISE couple 2, optimal scheme in
443 blue

CO ₂ -ISEcouple 2		Slope (mV/decade)	Intercept (mV)	Drift (mv/s)
	1	27.30	-83.24	-
Calibration Type*	2	27.30	-70.23	0.010
	3	27.30	-68.85	0.009
	4	32.82	-43.46	0.003

444

445

446

447

(d) Calibration types and parameters for CO₂-ISE SH probe

CO ₂ -SH		Slope (mV/decade)	Intercept (mV)	Drift (mV/s)
	1	56.85	70.86	-
Calibration Type*	2	-	-	-
	3	56.85	98.31	0
	4	48.35	63.81	0

FIGURES

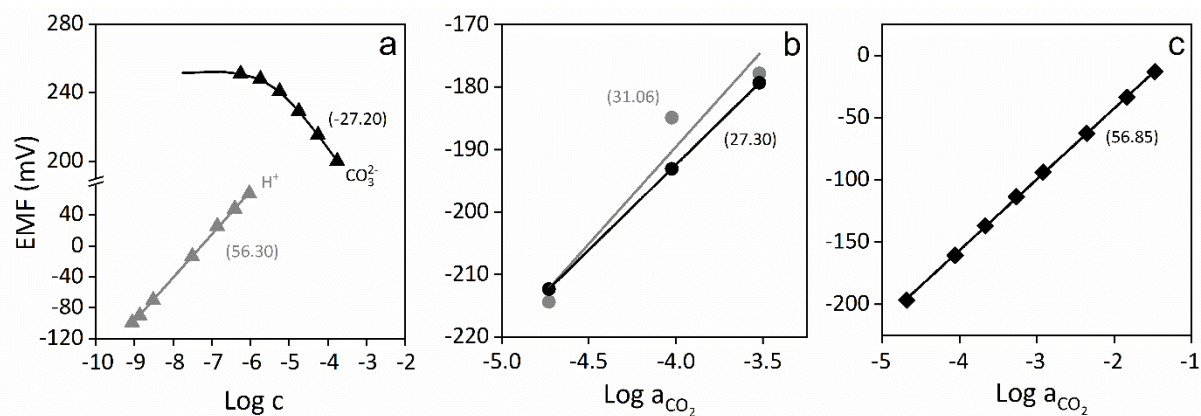


Figure 1. Response (with respective slopes in mV/decade reported in parentheses) of (a) carbonate and hydrogen ion selective SC-ISEs in the laboratory (b) CO_2 -ISE couples on board (c) CO_2 -SH probe before the deployment on change in dissolved CO_2 concentrations.

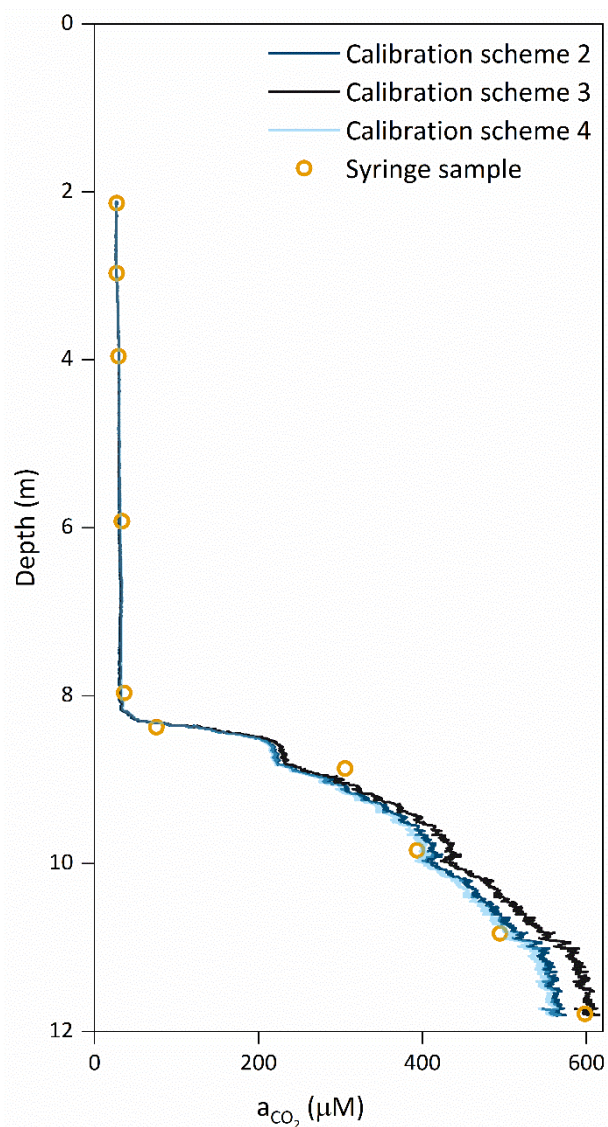


Figure 2. Depth profiles of activity of dissolved CO_2 obtained by CO_2 ISE couple calculated with different calibration parameters corresponding to the three *in situ* calibration schemes as described in Table 1. Please note that the dark blue line for scheme 2 is almost overlapped with the light blue line of scheme 4.

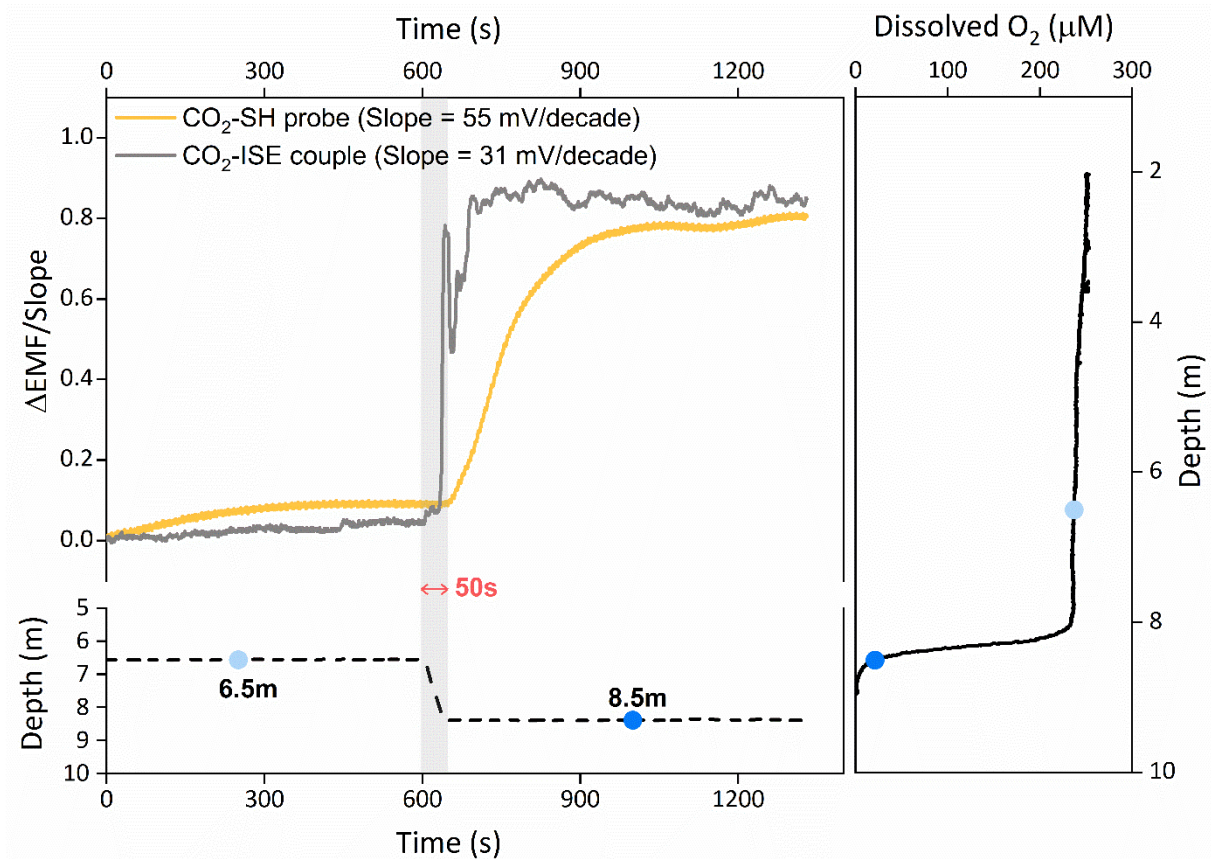


Figure 3. Temporal response of CO₂-SH probe and CO₂-ISE couple on fast profiling with 5cm/s (10 folds normal speed). Slopes for both type of sensors as per calibration scheme 3. The blue points on the dissolved oxygen profile and on the depth profile indicate the syringe sampling locations.

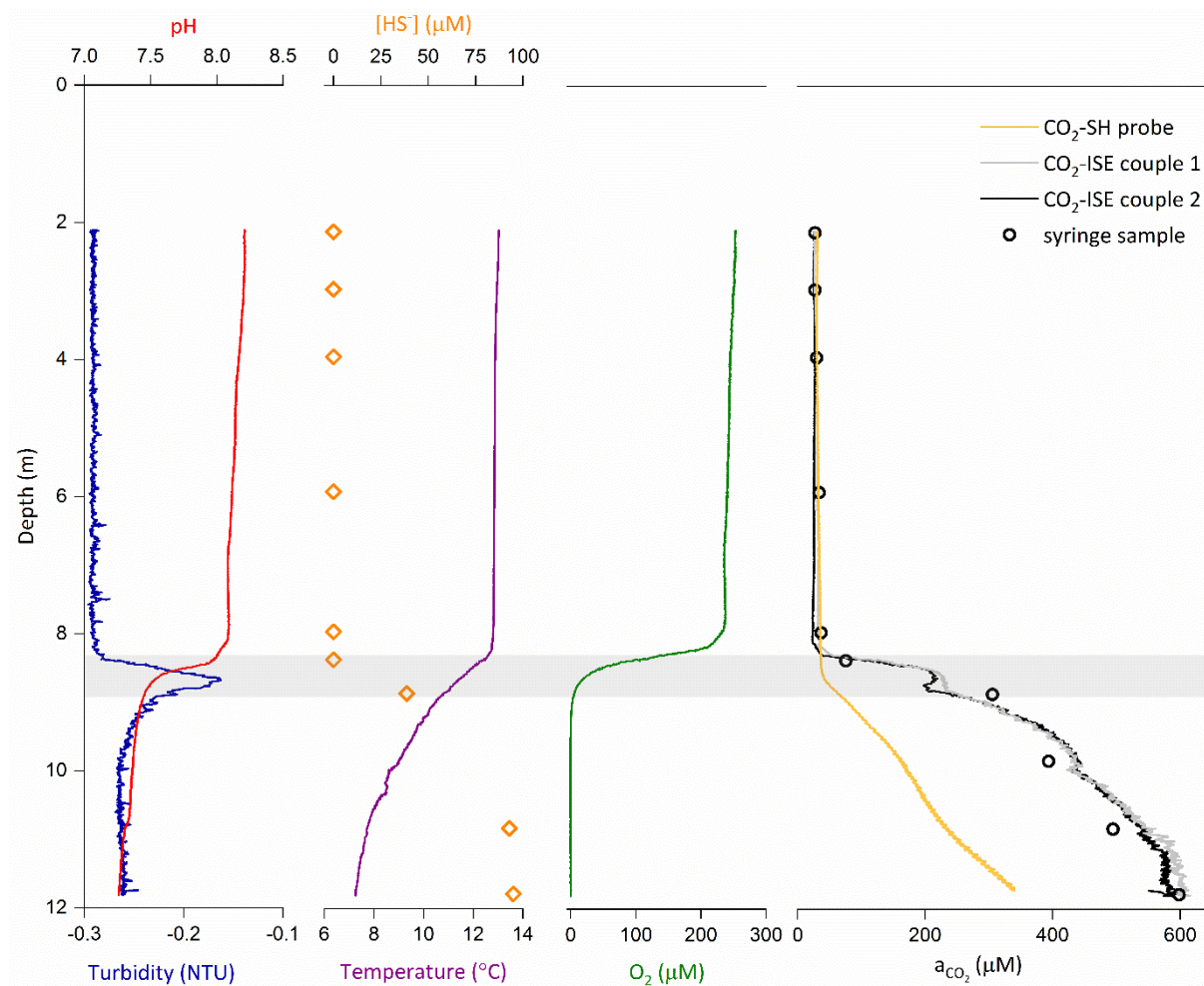


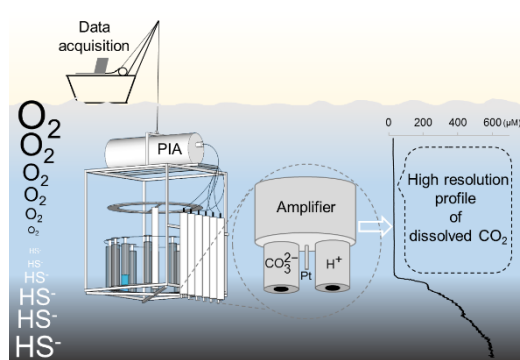
Figure 4. *In situ* high-resolution profiles of physicochemical characteristics of water column, activity of dissolved CO₂ by CO₂-ISE couples and a comparison with simultaneous response of CO₂-SH probe and syringe samples at profiling speed 0.5cm/s in Lake Rotsee.

492

493

TOC art

494



Supporting Information (SI) for

Fast Potentiometric CO₂ Sensor for High-resolution *In situ* Measurements in Fresh Water Systems

Rohini Athavale^{1, 2†*}, Nadezda Pankratova^{3, 4‡}, Christian Dinkel¹, Eric Bakker³, Bernhard Wehrli^{1, 2},
Andreas Brand^{1, 2}

¹Eawag – Swiss Federal Institute of Aquatic Science and Technology, Department of Surface Waters Research and Management, Seestrasse 79, CH-6047 Kastanienbaum, Switzerland.

²Institute of Biogeochemistry and Pollutant Dynamics, ETH Zurich, Universitätsstrasse 16, CH-8092 Zürich, Switzerland.

³Department of Inorganic and Analytical Chemistry, University of Geneva, Quai E.-Ansermet 30, 1211 Geneva, Switzerland.

⁴Integrated Systems Laboratory (LSI), Swiss Federal Institute of Technology Lausanne (EPFL), CH-1015 Lausanne, Switzerland.

^{†‡} Both authors contributed equally

*Corresponding Author

E-mail: rohini.athavale@eawag.ch

Phone Number: +41 587655633

TABLE OF CONTENTS

24 **EXPERIMENTAL SECTION**

25 Materials and Chemicals

26 Synthesis of f-MWCNTs

27 Sensor fabrication

28 Laboratory tests

29

30 **TABLES SI**

31 Selectivity coefficients for both SC-ISEs for relevant interfering ions and their respective mean
32 concentrations (Table S1)

33 Sensor performance during all the described laboratory test (Table S2)

34

35 **FIGURES SI**

36 Sulfide insensitivity test (Figure S1)

37 Depth profile of raw and drift corrected Δ EMF (Figure S2)

38 Depth profiles of activity of dissolved CO₂ obtained by CO₂-SH probe obtained with different
39 calibration schemes (Figure S3)

40 Custom built profiling ion analyzer (PIA) set up with integrated commercial sensors, syringe
41 sampler and the developed SC-ISE set up for dissolved CO₂ (Figure S4)

42

43

44 **EXPERIMENTAL SECTION**

45 *Materials and Chemicals*

46 The following reagents were purchased in selectophore grade from Sigma-Aldrich: potassium
47 tetrakis(4-chlorophenyl)borate (KTPCIPB), tri-n-dodecylamine(TDDA), tetrahydrofuran
48 (THF), N,N-dioctyl-3 α ,12 α -bis(4-trifluoroacetylbenzoyloxy)-5 β -cholan-24-amide (carbonate
49 ionophore VII), bis(2-ethylhexyl) adipate (DOA), tridodecylmethylammonium chloride
50 (TDMACl). Poly(vinyl-chloride) (PVC, high molecular weight), octadecyl amine (ODA),
51 methylene chloride(CH₂Cl₂), thionyl chloride (SOCl₂), potassium hexacyanoferrate(II)
52 trihydrate (K₄Fe(CN)₆.3H₂O), potassium hexacyanoferrate(III) (K₃Fe(CN)₆), sodium sulfide
53 nonahydrate (Na₂S.9H₂O), zinc acetate (Zn(CH₃COO)₂), sodium carbonate (Na₂CO₃), N,N-
54 Dimethyl-1,4-phenylenediammonium dichloride (C₈H₁₂N₂.2HCl), ammonium iron (III) sulfate
55 (NH₄Fe(SO₄)₂.12H₂O, nitric acid (HNO₃), and hydrochloric acid (HCl), were obtained in
56 analytical grade from Sigma-Aldrich. Biology grade 2-amino-2-hydroxymethyl-propane-1,3-
57 diol (Tris base) was was purchased from Promega corporation, USA. Multiwall carbon
58 nanotubes (MWCNTs) (0.5-200 μ m length and 30-50 nm diameter, M4905) were obtained
59 from HeJi Inc. The methacrylic copolymer (MMA-DMA) was synthesized in the research
60 group of Prof. Eric Bakker, University of Geneva, according to the protocol by Heng et al.¹
61 Aqueous solutions were prepared by dissolving appropriate salts or diluting standard solutions
62 in nano-pure water with a resistance of 18.2 M Ω cm⁻¹. A double junction Ag/AgCl reference
63 electrode (Metrohm AG, Switzerland) containing 3M KCl as an inner solution and 1M
64 CH₃COOLi as a bridge electrolyte was used for the lab experiments.

65 *Synthesis of f-MWCNT*

66 MWCNTs were functionalized by following the protocol of Crespo et. al.² Briefly, 1 g of
67 MWCNTs were refluxed for an hour at 100 °C in H₂SO₄/HNO₃ (3:1). The resultant MWCNT-
68 COOH were then filtered through a Polycarbonate (0.10 μ m) membrane, followed by washing
69 with nanopure water and drying at 60°C. Further, 20 ml of thionyl chloride (SOCl₂) and 1 ml
70 of dimethylformamide was added and the mixture was refluxed overnight, at 70°C. After the

reaction, the residual solvent was removed by rotary evaporation. Finally, an excess of ODA (~1g) was added and the mixture was continuously stirred at 100°C for 96 h. After cooling to room temperature, the excess ODA was removed by sonication and several washing steps with ethanol. The resultant carbon nanotubes were then dried and stored at room temperature.

Preparation of f-MWCNT based SC-ISE for H^+ and CO_3^{2-}

A stable dispersion of nanotubes was achieved by simply sonicating 1mg f-MWCNTs in 1 ml THF for ~10 minutes. For preparation of SC-ISEs 100 μ l of this dispersion was drop casted on a preferentially masked GC electrode surface to form a uniform layer. New mask was prepared for each GC electrode using a simple method where, pieces of a Scotch® tape (Scotch™3M, USA) were stuck on top of each other taking care that no air is trapped to obtain a ~0.6 mm thick band. This band was punched with a punching machine for desired sized hole so as to cover the glassy carbon surface and mask the surrounding inert surface of the electrode body. The hydrogen ion-selective membrane cocktail was prepared by dissolving 1.95 mg TDDA, 0.58 mg KTpClPB and 97.47 mg MMA-DMA in 1 mL dichloromethane and for the carbonate ion selective membrane 8.3 mg carbonate ionophore VII, 2 mg TDMAC, 60mg PVC and 100 μ L DOA were dissolved in 2mL THF. The mixture was sonicated for 30 s. Then, 130 μ L of the membrane cocktail was drop-cast onto the f-MWCNT layer that was previously deposited onto the glassy carbon surface.

Laboratory tests

Electrodes were conditioned before calibration by immersing carbonate selective SC-ISE in 10^{-4} M CO_3^{2-} for 1 day followed by 1 μ M solution for 1 day. For H^+ selective electrodes in the first conditioning step was pH 3 solution for 1 day followed by a second step in pH 9 solution for 2 days. During the lab experiments, a 16-channel EMF potentiometer (Lawson Labs Inc, USA) was used to record EMF.

Total sulfide in the samples was analyzed spectrophotometrically.³ The sampling procedure involved fixing total sulfide in the samples by adding 0.5 mL 4% zinc acetate solution to 1 mL unfiltered sample immediately after retrieving from the syringes. Sulfide standard solution (0.1M) was prepared with sodium sulfide nonahydrate in nanopure water. Standards were also treated with zinc acetate to fix total sulfide to zinc sulfide. The samples and standards were treated with an acidic solution of (~40% sulfuric acid) N,N-Dimethyl-1,4-phenylenediammonium dichloride and ammonium iron (III) sulfate to produce a blue color after 30 min incubation at room temperature. Both standard and samples were quantified for total sulfide at 665 nm.

Tris buffer preparation

10 mM Tris solution was prepared with 5 mM HCO_3^- , 150 μM NaCl in nanopure water and the pH was adjusted using sulfuric acid to 7.42, 7.98 and 8.64. The activity of CO_2 was calculated by defining the pH value, the concentration of HCO_3^- and Cl^- and the temperature as input to the speciation program PHREEQC.⁴

Sulfide sensitivity test

A sulfide sensitivity test was performed in a 100 mM Tris buffer at pH 8.2 (adjusted with H_2SO_4) with 1 mM total carbonate. The sulfide concentration was adjusted by incremental addition of a sodium sulfide solution.

Redox sensitivity test

A redox sensitivity test was performed in a 100 mM Tris buffer at pH 8.2 (adjusted with H_2SO_4) with 1 mM total carbonate for carbonate selective electrode and in an unbuffered background with 1mM H^+ for hydrogen ion selective electrode. The redox sensitivity was tested by measuring potential in a solution with 1 mM total concentration of $[\text{Fe}(\text{CN})_6]^{4-}/[\text{Fe}(\text{CN})_6]^{3-}$ redox couple. The concentration ratios of the redox couple ranging from 1/10 to 10/1.⁵

Water layer test

Water layer tests were carried out as described in Fibbioli et al.⁶ Before the water layer test, SC-ISEs were conditioned in respective primary ion solution (10^{-4} M CO_3^{2-} in Tris buffer pH 8.2 and H^+) solution and replaced by 1mM interfering ion (Cl^- at pH 8.2 and K^+ respectively) during the course of experiment and introduced again in 1mM primary ion solution.

TABLES SI

Table S1 Selectivity coefficients as determined by previous studies for H^+ sensitive membranes by FIM⁷ and for carbonate ion by SSM² mean concentration of possible interfering ions observed in the water column of Lake Rotsee during the in situ application

Interfering ion (b)	Selectivity coefficient $K_{\text{H}^+, \text{b}}^{\text{pot}}$	Selectivity coefficient $K_{\text{CO}_3^{2-}, \text{b}}^{\text{pot}}$	Mean concentration (M)
K^+	1.30×10^{-8}	-	3.90×10^{-5}
Na^+	1.10×10^{-9}	-	1.81×10^{-4}
Mg^{2+}	3.98×10^{-10}	-	1.87×10^{-4}
Ca^{2+}	4.36×10^{-9}	-	1.075×10^{-3}
Cl^-	-	1.58×10^{-7}	1.66×10^{-4}
NO_3^-	-	3.16×10^{-5}	3.00×10^{-6}

Table S2 Sensor performance respect to detection limits, long-term stability and tests for water layer and redox sensitivity.

Sensor type	Detection limit	Long term stability ^a	Water layer test	Redox sensitivity
-------------	-----------------	----------------------------------	------------------	-------------------

	(M)	Drift (mV/h)		(mV/decade)
Carbonate (CO_3^{2-})	2.0×10^{-6}	0.09	No drift	0.04
Hydrogen ion (H^+)	1.0×10^{-9}	0.06	No drift	0.05

^a Long term stability tests were performed in 10^{-3} M H^+ and 10^{-4} M of CO_3^{2-} solution for hydrogen and carbonate sensitive SC ISE respectively.

FIGURES S1

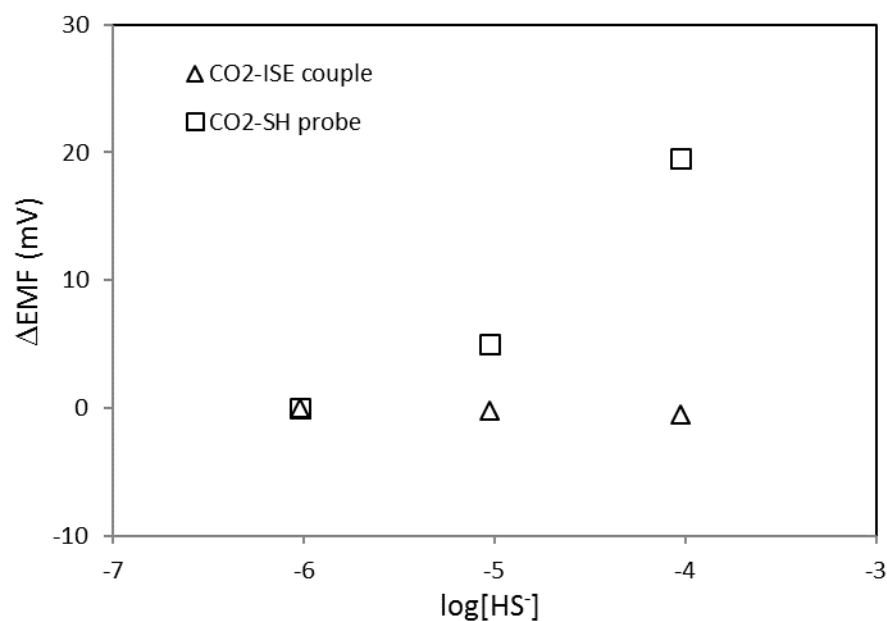


Figure S1 Sulfide insensitivity test for CO_2 -ISE couple compared to a CO_2 -SH probe in a buffered solution at pH 8.2

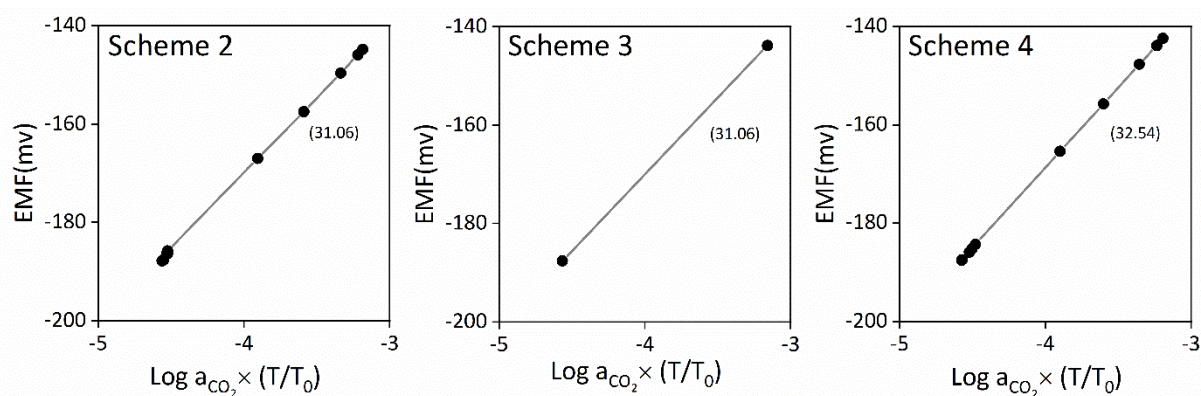


Figure S2 Schemes in optimization of *in situ* calibration where drift corrected EMF is

plotted against logarithm of activity of dissolved carbon dioxide multiplied with a temperature factor to obtain values of respective temperature corrected slopes in mv/decade(in parentheses) for ISE couple 1 (Refer to Table 1b in the main text).

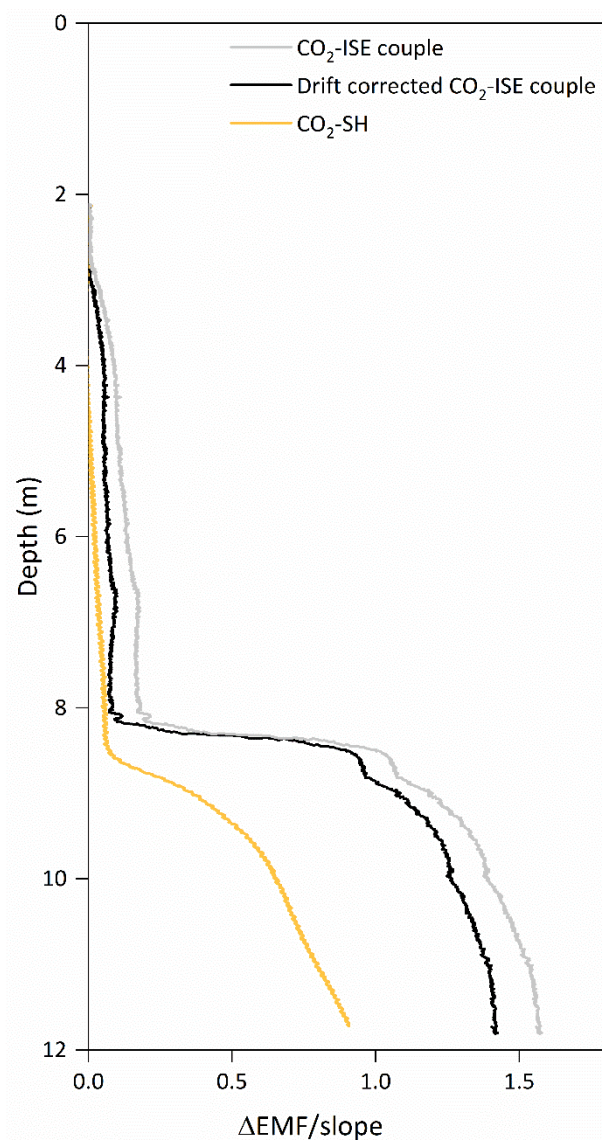


Figure S3 Depth profile of raw and drift corrected ΔEMF showing effect of drifting behavior of an ISE-couple on estimation of dissolved CO_2 concentration.

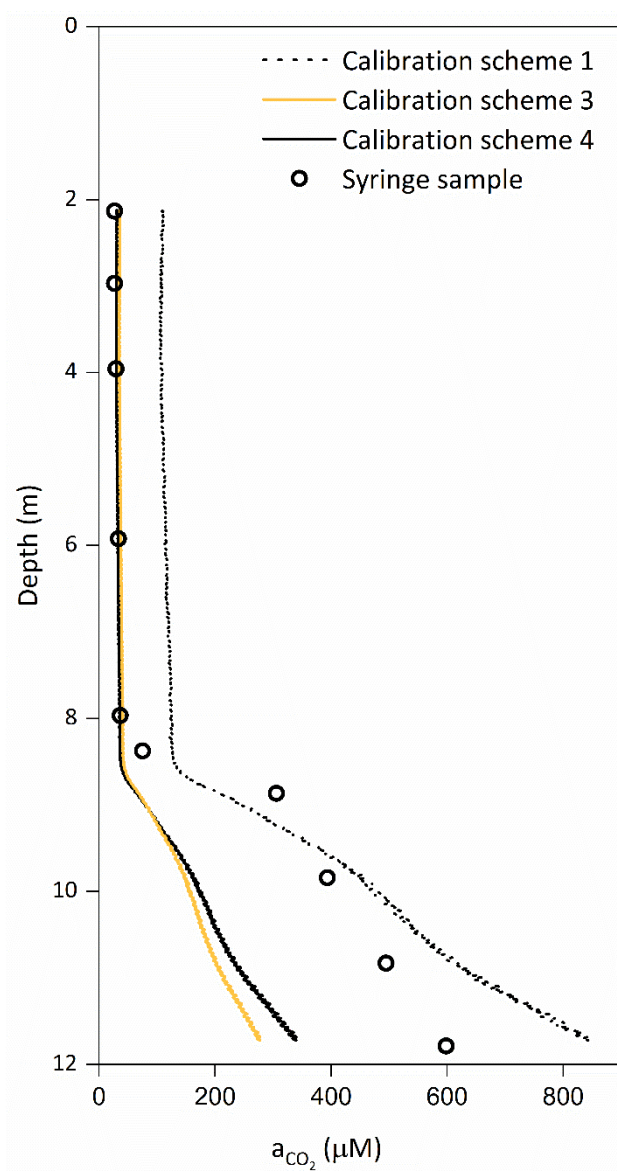


Figure S4 Depth profiles of activity of dissolved CO₂ obtained by CO₂-SH probe calculated with different calibration parameters corresponding to the calibration schemes as described in Table 1.

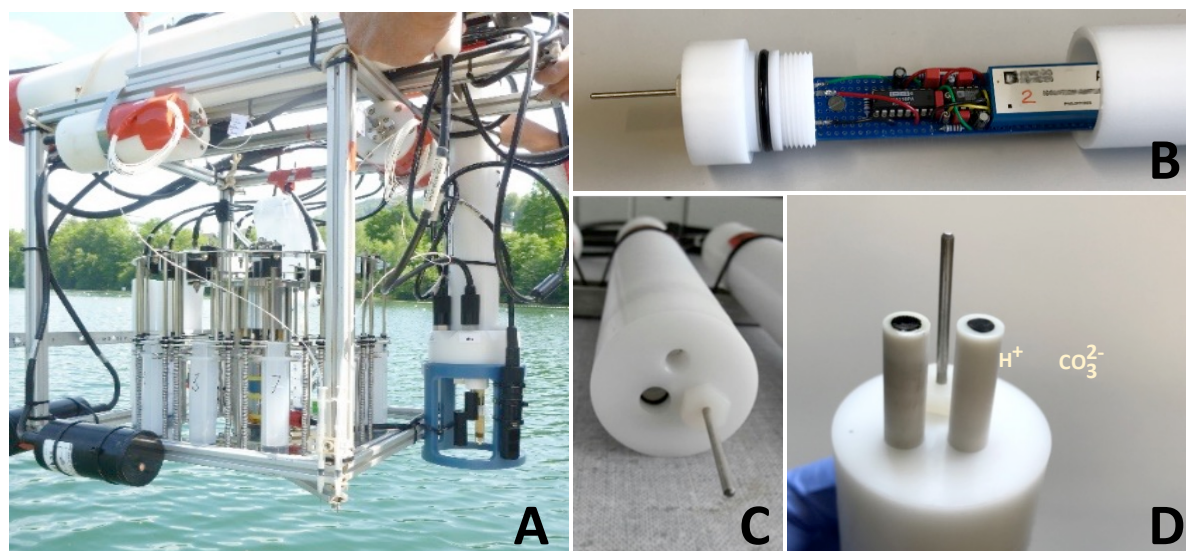


Figure S5 Profiling ion analyzer (PIA) a custom-built profiling set up that accommodates a syringe sampler, commercial sensors for physicochemical characterization of the water column (A) and waterproof amplifiers that house SC-ISEs (B, C) with SC-ISEs for hydrogen ion and carbonate installed (D) for *in situ* measurements of dissolved CO₂ in the water column.

REFERENCES

- Heng, L. Y.; Hall, E. A. H., Methacrylic–acrylic polymers in ion-selective membranes: achieving the right polymer recipe. *Anal Chim Acta* **2000**, *403*, (1–2), 77-89.
- Yuan, D.; Anthis, A. H. C.; Ghahraman Afshar, M.; Pankratova, N.; Cuartero, M.; Crespo, G. A.; Bakker, E., All-Solid-State Potentiometric Sensors with a Multiwalled Carbon Nanotube Inner Transducing Layer for Anion Detection in Environmental Samples. *Analytical chemistry* **2015**, *87*, (17), 8640-8645.
- Cline, J. D., Spectrophotometric Determination of Hydrogen Sulfide in Natural Waters. *Limnol Oceanogr* **1969**, *14*, (3), 454-458.
- Parkhurst, D. L., *User's guide to PHREEQC : a computer program for speciation, reaction-path, advective-transport, and inverse geochemical calculations*. Lakewood, Colo. : U.S. Dept. of the Interior, U.S. Geological Survey ; Denver, CO : Earth Science Information Center, Open-File Reports Section [distributor], 1995.: 1995.
- Mousavi, Z.; Teter, A.; Lewenstam, A.; Maj-Zurawska, M.; Ivaska, A.; Bobacka, J., Comparison of Multi-walled Carbon Nanotubes and Poly(3-octylthiophene) as Ion-to-Electron Transducers in All-Solid-State Potassium Ion-Selective Electrodes. *Electroanal* **2011**, *23*, (6), 1352-1358.
- Fibbioli, M.; Morf, W. E.; Badertscher, M.; de Rooij, N. F.; Pretsch, E., Potential drifts of solid-contacted ion-selective electrodes due to zero-current ion fluxes through the sensor membrane. *Electroanal* **2000**, *12*, (16), 1286-1292.
- Crespo, G. A.; Gugsá, D.; Macho, S.; Rius, F. X., Solid-contact pH-selective electrode using multi-walled carbon nanotubes. *Anal Bioanal Chem* **2009**, *395*, (7), 2371-2376.